



## Phase equilibria and crystal structure of the complex oxides in the Sr–Fe–Co–O system

T.V. Aksenova, L.Ya. Gavrilova, V.A. Cherepanov\*

Ural State University, Lenin av. 51, Yekaterinburg 620083, Russia

### ARTICLE INFO

#### Article history:

Received 15 November 2007

Received in revised form

14 March 2008

Accepted 14 March 2008

Available online 21 March 2008

#### Keywords:

Phase diagram

Crystal structure

Solid solution

X-ray diffraction

Thermogravimetric analysis

### ABSTRACT

Phase relations in the Sr–Fe–Co–O system have been investigated at 1100 °C in air by X-ray powder diffraction on quenched samples. Solid solutions of the form  $\text{SrFe}_{1-x}\text{Co}_x\text{O}_{3-\delta}$  ( $0 \leq x \leq 0.7$ ),  $\text{Sr}_3\text{Fe}_{2-y}\text{Co}_y\text{O}_{7-\delta}$  ( $0 \leq y \leq 0.4$ ) and  $\text{Sr}_4\text{Fe}_{6-z}\text{Co}_z\text{O}_{13\pm\delta}$  ( $0 \leq z \leq 1.6$ ) were prepared by solid-state reaction and by the sol–gel method. The structural parameters of single-phase samples were refined by the Rietveld profile method. The variation of the lattice parameters with composition has been determined for each solid solution and a cross-section of the phase diagram at 1100 °C in air for the entire Sr–Fe–Co–O system has been constructed.

© 2008 Elsevier Inc. All rights reserved.

### 1. Introduction

Strontium iron oxides, especially those doped with cobalt, in which ionic and electronic conductivity coexist, received much interest because of their potential applications for oxygen separating membranes and for the partial oxidation of methane [1]. Extensive studies of preparation routes for particular compositions, structure and physical properties have been carried out in recent years [2–6]. The magnetic properties of these oxides have also received special attention because of the MR effect in  $\text{Sr}_3\text{Fe}_{2-y}\text{Co}_y\text{O}_{7-\delta}$  and  $\text{SrFe}_{1-x}\text{Co}_x\text{O}_{3-\delta}$  [7–10]. Relatively little work, however, has been done on the phase stability or phase equilibria in the Sr–Fe–Co–O system [11–13].

The binary oxides  $\text{SrFeO}_{3-\delta}$ ,  $\text{Sr}_2\text{FeO}_{4-\delta}$ ,  $\text{Sr}_4\text{Fe}_3\text{O}_{10-\delta}$ ,  $\text{Sr}_3\text{Fe}_2\text{O}_{7-\delta}$ ,  $\text{Sr}_4\text{Fe}_6\text{O}_{13\pm\delta}$  and  $\text{SrFe}_{12}\text{O}_{19}$  in the Sr–Fe–O system have been described in Refs. [14–28]. Several oxides with 1:1 Sr:Fe ratio with varying oxygen content and different crystal structures are known [14–21]. The oxygen content and stability of these oxides depends on the temperature and oxygen partial pressure in an ambient atmosphere. X-ray diffraction (XRD) data show that  $\text{SrFeO}_{3-\delta}$  has an ideal cubic structure when  $2.88 \leq (3-\delta) \leq 3$  [15,17,20], a tetragonal structure at  $2.76 \leq (3-\delta) \leq 2.84$  [15,16,19], an orthorhombic structure when  $(3-\delta) = 2.75$  [15,16,18] and a brownmillerite structure when  $(3-\delta) = 2.5$  [17,21]. Takeda and Watanabe [29] prepared a continuous series of solid solutions  $\text{SrFe}_{1-x}\text{Co}_x\text{O}_{3-\delta}$  ( $0 \leq x \leq 1$ ), which were heat-treated above 1000 °C,

quenched and then heat-treated below 450 °C at high oxygen pressure. The resulting samples possessed cubic perovskite-type structure, in good agreement with the results reported in [17].

$\text{Sr}_2\text{FeO}_{4-\delta}$  synthesized at 750 °C under the flowing oxygen (200 atm), crystallizes with a tetragonal unit cell ( $I4/mmm$  space group):  $a = 3.864 \text{ \AA}$ ,  $c = 12.397 \text{ \AA}$  [22]. Heating above  $930 \pm 10 \text{ °C}$  leads to decomposition of  $\text{Sr}_2\text{FeO}_{4-\delta}$  to  $\text{Sr}_3\text{Fe}_2\text{O}_{7-\delta}$  and SrO [14,22]. Strontium ferrite  $\text{Sr}_4\text{Fe}_3\text{O}_{10-\delta}$ , like  $\text{Sr}_2\text{FeO}_{4-\delta}$ , is unstable under heating and decomposes into  $\text{Sr}_3\text{Fe}_2\text{O}_{7-\delta}$  and  $\text{SrFeO}_{3-\delta}$  above  $850 \pm 25 \text{ °C}$  [14].

Tetragonal oxygen-deficient  $\text{Sr}_3\text{Fe}_2\text{O}_{7-\delta}$  has been prepared by the conventional ceramic technique at 1100 °C in air with following annealing at 900 °C in flowing  $\text{O}_2$  [23]. According to [7], single-phase  $\text{Sr}_3\text{Fe}_{2-y}\text{Co}_y\text{O}_{7-\delta}$  exists in the range  $0.25 \leq y \leq 1.75$  when prepared at 1000 °C under flowing oxygen. The X-ray patterns of all samples show that these solid solutions are isostructural with the parent compound  $\text{Sr}_3\text{Fe}_2\text{O}_{7-\delta}$ .

The incommensurate modulated structure of  $\text{Sr}_4\text{Fe}_6\text{O}_{13\pm\delta}$ , refined from single-crystal XRD data by the super-space formalism, is described in [24]. A single crystal was treated at 1430 °C for 4 h, the temperature was then lowered to 800 at 2 °C/h and finally reduced to room temperature in 12 h [24]. A precise structural characterization of the  $\text{Sr}_4\text{Fe}_6\text{O}_{13\pm\delta}$  system has been carried out by Rossell et al. [25], who found various space groups, depending on the oxygen content. The pseudo-binary phase diagram  $\text{Sr}_4\text{Fe}_6\text{O}_{13\pm\delta}$ – $\text{Sr}_4\text{Co}_6\text{O}_{13\pm\delta}$  in air has been studied by Fossdal et al. [11]. They find that  $\text{Sr}_4\text{Fe}_6\text{O}_{13\pm\delta}$  is stable in air above  $775 \pm 25 \text{ °C}$ . The homogeneity range of  $\text{Sr}_4\text{Fe}_{6-z}\text{Co}_z\text{O}_{13\pm\delta}$  in air extended from  $z = 0$  to 0.9 at 1100 °C. These results conflict with the values  $0 \leq z \leq 1.8$  in [5,30] and with  $0 \leq z \leq 1.5$  in [31]. Undoped

\* Corresponding author. Fax: +7 3432 507401.

E-mail address: [Vladimir.Cherepanov@usu.ru](mailto:Vladimir.Cherepanov@usu.ru) (V.A. Cherepanov).

$\text{Sr}_4\text{Fe}_6\text{O}_{13}$  and the solid solution  $\text{Sr}_4\text{Fe}_{6-z}\text{Co}_z\text{O}_{13\pm\delta}$  possesses orthorhombic structure (*Iba2* space group) [25,30].

The crystal structure and some thermochemical properties of hexagonal  $\text{SrFe}_{12}\text{O}_{19-\delta}$  are described in [26–28]. The material was prepared as single crystals by the flux method [26,27] and in powder form by the citrate–nitrate gel combustion route, with final annealing at 1473 K in dry air for 100 h [28].

The phase equilibria and crystal structures of the single phases in the  $\text{CoO–Fe}_2\text{O}_3$  system were described in [32]. The homogeneity ranges in air at 1100 °C were found to be  $0 \leq x \leq 0.15$  for  $\text{Co}_{1-x}\text{Fe}_x\text{O}$  (sp. gr. *Fm3m*),  $0 \leq y \leq 0.03$  for  $\text{Fe}_{2-y}\text{Co}_y\text{O}_3$  and  $0.84 \leq z \leq 1.38$  for  $\text{Fe}_{3-z}\text{Co}_z\text{O}_4$ .

The present work is a study of the phase equilibria in the  $\text{Sr–Fe–Co–O}$  system in air at 1100 °C. The homogeneity ranges and crystal structures have been determined and a cross-section of the phase diagram has been constructed.

## 2. Experimental

Our starting materials were strontium carbonate  $\text{SrCO}_3$  of “special purity” grade, iron oxide  $\text{Fe}_2\text{O}_3$  of “pure for analysis” grade, cobalt oxide  $\text{Co}_3\text{O}_4$  of “pure for analysis” grade and metallic iron of “pure for analysis” grade. All materials were preliminarily dried in air to remove adsorbed moisture and gases:  $\text{SrCO}_3$  and  $\text{Co}_3\text{O}_4$  at 600 °C for 3 h, and  $\text{Fe}_2\text{O}_3$  at 500 °C for 3 h. The metallic cobalt was obtained by reducing  $\text{Co}_3\text{O}_4$  in flowing hydrogen at 600 °C.

Several samples were prepared by solid-state reaction in air at temperatures between 850 and 1100 °C for 240–316 h, with intermediate grindings. Other samples were synthesized by the sol–gel methods. Appropriate amounts of  $\text{SrCO}_3$ , metallic Fe and Co were dissolved in nitric acid, and then either crystalline citric acid hydrate or glycerin was added to the solution. The resulting gel was dried, decomposed at 300 °C and calcined at various temperatures (400–1100 °C) in air for 72–120 h, with intermediate grindings.

Obtained oxides were characterized by XRD using DRON-UM1 diffractometers with  $\text{CuK}\alpha$  radiation. A pyrolytic graphite monochromator was used for the reflected beam ( $\lambda = 1.5418 \text{ \AA}$ ). Silicon was used as the external standard. The full-profile Rietveld analysis (“Fullprof 2006”) was used for the crystal structure refinement. Intensity data were collected point by point over the angular range  $10^\circ \leq 2\theta \leq 70^\circ$ , with  $0.02^\circ$  steps for 1–10 s. Convergence between experimental XRD data and the calculated profile was estimated by a set of standard factors:  $R_{\text{wp}}$ —the weighed profile factor,  $R_p$ —the profile factor,  $R_f$ —the structural factor,  $R_{\text{Br}}$ —the Bragg-factor and  $R_{\text{exp}}$ —the expected factor.

Oxygen content in some samples was determined by reduction at hydrogen flux in TGA equipment at 1100 °C. X-ray powder diffraction of the samples after reduction confirms that only SrO, Fe and Co were present as the products. The accuracy of the oxygen content determination was within  $\pm 0.01$ .

## 3. Results and discussion

The phase equilibria in the  $\text{Sr–Fe–Co–O}$  system were studied at 1100 °C in air using 68 samples with various compositions.

### 3.1. Solid solution $\text{SrFe}_{1-x}\text{Co}_x\text{O}_{3-\delta}$

In order to determine the homogeneity range of the solid solution  $\text{SrFe}_{1-x}\text{Co}_x\text{O}_{3-\delta}$ , samples with  $x = 0, 0.1, 0.2, 0.3, 0.4, 0.5, 0.6, 0.7, 0.8, 0.9, 0.95$  and 1 were prepared. The syntheses were performed by the citrate–nitrate and standard ceramic

techniques. The tetragonal unit cell parameters of the ferrite  $\text{SrFeO}_{3-\delta}$  obtained in the present work ( $a = 10.945(1) \text{ \AA}$ ,  $c = 7.705(1) \text{ \AA}$ ) are in a good agreement with those reported earlier [15,16]. The TGA results indicate that the oxygen content in  $\text{SrFeO}_{3-\delta}$  at 1100 °C in air was determined as  $2.52 \pm 0.01$  ( $\delta = 0.48 \pm 0.01$ ), which agrees with the value reported in [18] under the same conditions. The XRD results for quenched samples show that single-phase solid solutions  $\text{SrFe}_{1-x}\text{Co}_x\text{O}_{3-\delta}$  forms at 1100 °C in air within the range  $0 \leq x \leq 0.7$ . Beyond this range  $\text{SrCo}_{2.5\pm\delta}$  was detected as a second phase. The crystal structure of the  $\text{SrFe}_{1-x}\text{Co}_x\text{O}_{3-\delta}$  with cobalt content  $0 \leq x \leq 0.3$  was found to be tetragonal, space group *I4/mmm*. Further substitution of iron for cobalt in crystal structure led to the change of lattice symmetry: solid solutions with  $0.3 \leq x \leq 0.7$  have a cubic structure, space group *Pm3m*. The oxygen deficiency, determined by TGA in  $\text{SrFe}_{0.5}\text{Co}_{0.5}\text{O}_{3-\delta}$  is  $0.44 \pm 0.01$ . The XRD pattern and the refined Rietveld profile for single-phase  $\text{SrFe}_{0.3}\text{Co}_{0.7}\text{O}_{3-\delta}$  are shown in Fig. 1. The unit cell parameters for  $\text{SrFe}_{1-x}\text{Co}_x\text{O}_{3-\delta}$  are listed in Table 1. Cobalt substitution for iron in  $\text{SrFe}_{1-x}\text{Co}_x\text{O}_{3-\delta}$  ( $0.3 \leq x \leq 0.7$ ) decreases the parameter  $a$  (Fig. 2) and hence the volume of unit cell, since ionic radius for cobalt ion ( $r(\text{Co}^{3+}) = 0.685$ ;  $r(\text{Co}^{4+}) = 0.67 \text{ \AA}$ ) is smaller than that for iron ion ( $r(\text{Fe}^{3+}) = 0.785$ ;  $r(\text{Fe}^{4+}) = 0.725 \text{ \AA}$ ) [33].

### 3.2. Solid solution $\text{Sr}_3\text{Fe}_{2-y}\text{Co}_y\text{O}_{7-\delta}$

The samples of general composition  $\text{Sr}_3\text{Fe}_{2-y}\text{Co}_y\text{O}_{7-\delta}$  with  $y = 0, 0.1, 0.2, 0.3, 0.4, 0.5, 0.6, 0.7, 0.8, 0.9, 1, 1.2, 1.4$  were prepared by the citrate–nitrate method. The homogeneity range of the solid solutions  $\text{Sr}_3\text{Fe}_{2-y}\text{Co}_y\text{O}_{7-\delta}$  was found to be  $0 \leq y \leq 0.4$ . The XRD patterns of the samples with  $0.4 \leq y \leq 1.4$  revealed additional reflections from  $\text{Sr}_3\text{Co}_2\text{O}_{7-\delta}$ . The structure of undoped  $\text{Sr}_3\text{Fe}_2\text{O}_{7-\delta}$  at 1100 °C is tetragonal, with unit cell parameters  $a = 3.866(1) \text{ \AA}$ ,  $c = 20.162(1) \text{ \AA}$ , (*I4/mmm* space group). The lattice parameters, refined from XRD results, for single-phase tetragonal  $\text{Sr}_3\text{Fe}_{2-y}\text{Co}_y\text{O}_{7-\delta}$  are listed in Table 2. The profile obtained from the Rietveld analysis for unsubstituted  $\text{Sr}_3\text{Fe}_2\text{O}_{7-\delta}$  is shown in Fig. 3.

### 3.3. Solid solution $\text{Sr}_4\text{Fe}_{6-z}\text{Co}_z\text{O}_{13\pm\delta}$

Examination of annealed  $\text{Sr}_4\text{Fe}_{6-z}\text{Co}_z\text{O}_{13\pm\delta}$  samples with  $0 \leq z \leq 1.8$  shows that solid solutions exist in the range  $z = 0–1.6$ .

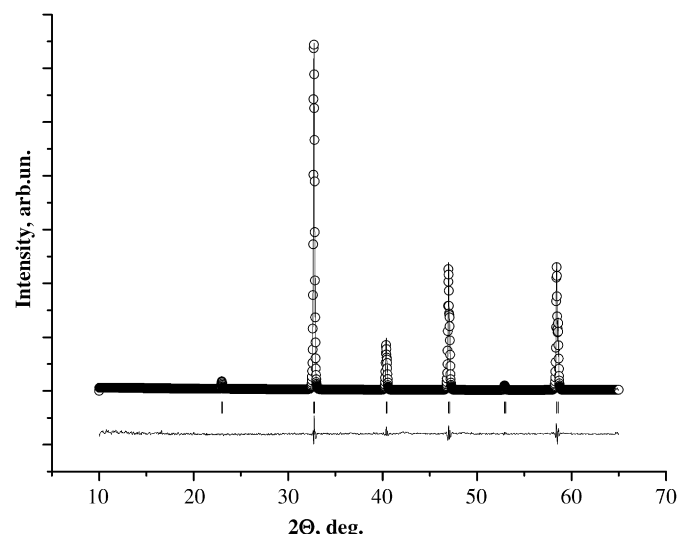
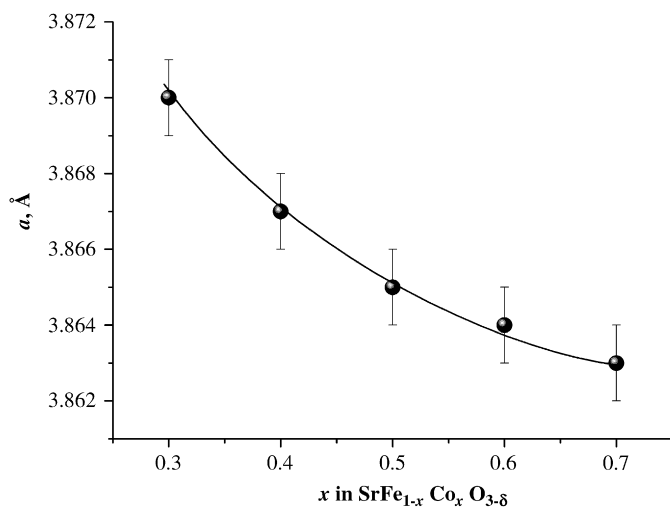


Fig. 1. Rietveld refinement profile for the single-phase solid solution  $\text{SrFe}_{0.3}\text{Co}_{0.7}\text{O}_{3-\delta}$ : open circles—experimental XRD data, upper continuous line is the calculated profile, lower continuous line is the difference plot.

**Table 1**  
Structural parameters for  $\text{SrFe}_{1-x}\text{Co}_x\text{O}_{3-\delta}$  solid solution quenched from 1100 °C in air

x	a (Å)	b (Å)	c (Å)	Refinement parameters		
				$R_{\text{Br}}$	$R_{\text{f}}$	$R_{\text{p}}$
<i>I4/mmm</i>						
0	10.945(1)	10.945(1)	7.705(1)	0.541	1.06	10.8
0.1	10.917(2)	10.917(2)	7.730(1)	0.745	1.50	12.2
0.2	10.920(1)	10.920(1)	7.734(1)	1.28	1.94	11.2
<i>Pm3m</i>						
0.3	3.870(1)	3.870(1)	3.870(1)	1.94	1.94	10.6
0.4	3.867(1)	3.867(1)	3.867(1)	4.90	4.98	14.0
0.5	3.865(1)	3.865(1)	3.865(1)	3.69	4.13	13.6
0.6	3.864(1)	3.864(1)	3.864(1)	5.20	5.88	14.3
0.7	3.863(1)	3.863(1)	3.863(1)	1.11	1.14	7.8



**Fig. 2.** The unit cell parameters for the solid solution  $\text{SrFe}_{1-x}\text{Co}_x\text{O}_{3-\delta}$ .

**Table 2**  
Structural parameters for  $\text{Sr}_3\text{Fe}_{2-y}\text{Co}_y\text{O}_{7-\delta}$  solid solution quenched from 1100 °C in air (*I4/mmm* space group)

x	a (Å)	c (Å)	V (Å <sup>3</sup> )	Refinement parameters		
				$R_{\text{Br}}$	$R_{\text{f}}$	$R_{\text{p}}$
0	3.867(1)	20.156(1)	301.37(2)	4.86	4.79	9.48
0.1	3.866(1)	20.152(2)	301.23(3)	1.93	1.56	9.71
0.2	3.863(1)	20.151(2)	300.82(2)	1.70	1.67	9.28
0.3	3.861(1)	20.155(1)	300.52(2)	0.845	0.915	9.08
0.4	3.859(1)	20.153(1)	300.13(2)	0.992	0.999	8.94

The preparation technique for each sample is appended to Table 3. The maximum value of Co substitution for Fe lies between  $z = 1.6$  and 1.7, which is slightly smaller the values reported in [5,11]. This can be explained by the fact that our samples were prepared at a higher temperature (1100 °C) than those used in [5,11] (850–900 °C). Our XRD pattern for  $\text{Sr}_4\text{Fe}_6\text{O}_{13\pm\delta}$  is identical to that reported in [5] (orthorhombic unit cell parameters  $a = 11.107(2)$  Å,  $b = 18.949(2)$  Å,  $c = 5.580(1)$  Å, space group *Iba2*). The introduction of cobalt into the structure of  $\text{Sr}_4\text{Fe}_{6-z}\text{Co}_z\text{O}_{13\pm\delta}$  leads to monotonic variations in the unit cell parameters with increase of cobalt content (Fig. 4). The volume of unit cell decreases with  $z$  because ionic radius of cobalt is smaller than that of iron. The unit cell parameters obtained for single-phase  $\text{Sr}_4\text{Fe}_{6-z}\text{Co}_z\text{O}_{13\pm\delta}$  are given in Table 3.

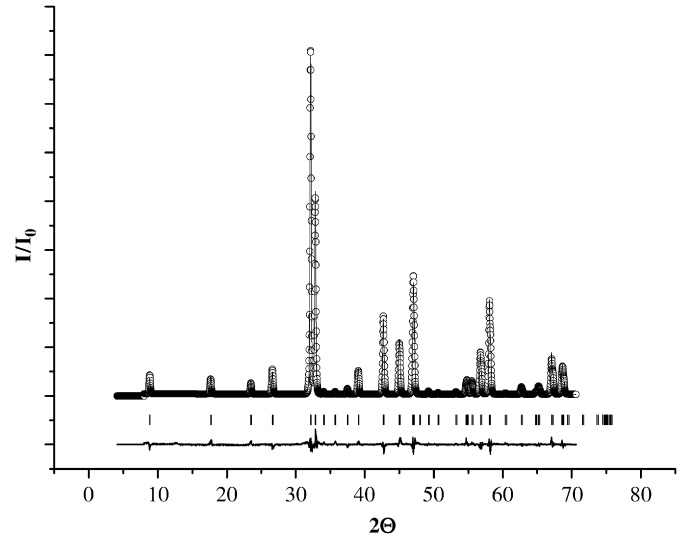


**Fig. 3.** Rietveld refinement profile for the single-phase  $\text{Sr}_3\text{Fe}_2\text{O}_{7-\delta}$ : open circles—experimental XRD data, upper continuous line is the calculated profile, lower continuous line is the difference plot.

**Table 3**  
Structural parameters for  $\text{Sr}_4\text{Fe}_{6-z}\text{Co}_z\text{O}_{13\pm\delta}$  solid solution quenched from 1100 °C in air (*Iba2* space group)

x	a (Å)	b (Å)	c (Å)	V (Å <sup>3</sup> )	Refinement parameters		
					$R_{\text{Br}}$	$R_{\text{f}}$	$R_{\text{p}}$
0 <sup>a</sup>	11.107(2)	18.949(2)	5.580(1)	1174.65(2)	1.61	1.47	12.1
0.1 <sup>b</sup>	11.103(1)	18.960(2)	5.578(1)	1174.43(2)	1.51	1.40	11.3
0.2 <sup>a</sup>	11.095(1)	18.960(2)	5.577(1)	1173.27(1)	1.75	2.85	10.6
0.3 <sup>b</sup>	11.081(1)	18.970(2)	5.572(1)	1171.06(2)	1.42	1.93	10.8
0.4 <sup>a</sup>	11.080(1)	18.977(2)	5.570(1)	1171.43(1)	1.63	1.80	10.5
0.6 <sup>a</sup>	11.062(1)	18.996(2)	5.565(1)	1169.48(1)	1.26	1.95	9.71
0.8 <sup>a</sup>	11.062(1)	18.987(2)	5.565(1)	1169.14(3)	1.37	1.77	10.6
1 <sup>a</sup>	11.061(1)	18.993(2)	5.565(1)	1169.63(2)	1.65	2.69	10.4
1.2 <sup>a</sup>	11.047(1)	19.000(2)	5.558(1)	1166.81(2)	1.34	1.63	10.6
1.4 <sup>a</sup>	11.038(1)	19.001(2)	5.554(1)	1165.06(3)	1.27	1.50	9.92
1.6 <sup>a</sup>	11.039(1)	19.006(2)	5.552(1)	1165.13(3)	1.29	1.31	10.7

<sup>a</sup> Samples obtained by the glycerin–nitrate technique.

<sup>b</sup> Samples obtained by the citrate–nitrate technique.

#### 3.4. Solid solution $\text{SrFe}_{12-u}\text{Co}_u\text{O}_{19-\delta}$

The citrate–nitrate route was used to prepare  $\text{SrFe}_{12}\text{O}_{19-\delta}$  and  $\text{SrFe}_{12-u}\text{Co}_u\text{O}_{19-\delta}$  with  $u = 0.1$ . Strontium hexaferrite  $\text{SrFe}_{12}\text{O}_{19-\delta}$  is isomorphous with the magnetoplumbite  $\text{BaFe}_{12}\text{O}_{19-\delta}$  (space group *P6<sub>3</sub>/mmc*). All reflections of single-phase  $\text{SrFe}_{12}\text{O}_{19-\delta}$  quenched from 1100 °C in air were indexed in the *P6<sub>3</sub>/mmc* space group. The hexagonal lattice parameters obtained for  $\text{SrFe}_{12}\text{O}_{19-\delta}$  were  $a = b = 5.878(2)$  Å,  $c = 23.045(3)$  Å, in good agreement with those obtained in [26,27]. According to X-ray data, the sample with overall composition  $\text{SrFe}_{11.9}\text{Co}_{0.1}\text{O}_{19-\delta}$  consisted of three phases:  $\text{SrFe}_{12}\text{O}_{19-\delta}$ ,  $\text{Sr}_4\text{Fe}_{6-z}\text{Co}_z\text{O}_{13\pm\delta}$  solid solution and  $\text{CoFe}_2\text{O}_4$ . We conclude any range of  $z$  for which  $\text{Sr}_4\text{Fe}_{6-z}\text{Co}_z\text{O}_{13\pm\delta}$  is homogeneous is significantly less than 0.1.

#### 3.5. Phase diagram of the Sr–Fe–Co–O system in air at 1100 °C

A convenient plane representation of the quaternary Sr–Fe–Co–O system can be made in triangular form if the composition is expressed in terms of the molar fraction of the metallic

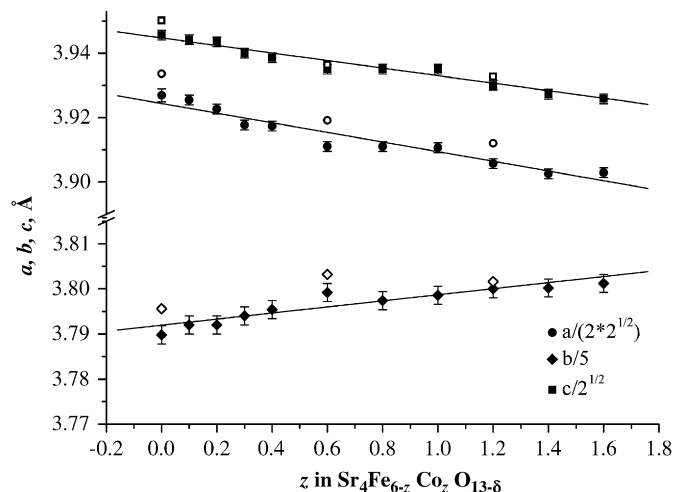


**Fig. 4.** The lattice parameters for  $\text{Sr}_4\text{Fe}_{6-z}\text{Co}_z\text{O}_{13-\delta}$  versus composition of solid solution: open symbols—data reported in [4], filled symbols—data obtained in this study.

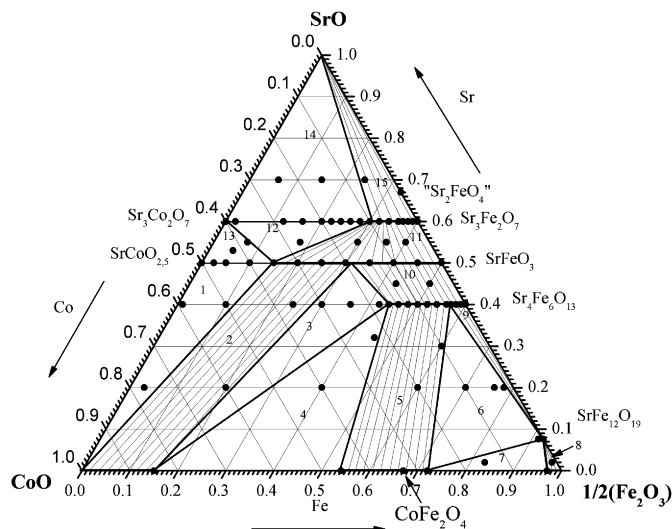


**Fig. 5.** Isobaric-isothermal cross-section of phase diagram of the Sr-Fe-Co-O system at 1100 °C in air.

components. However, the oxygen content in coexisting complex oxides cannot be determined from such a diagram, its value should be ascribed to the corresponding thermodynamically equilibrium composition of each phase.

Using the XRD data from all our samples, we have divided the isobaric-isothermal cross-section of the Sr-Fe-Co-O phase diagram into 15 phase fields (Fig. 5). The compositions of the samples are shown as points on the diagram. The phases coexisting in each field are given in Table 4. In field 3, semi-quantitative X-ray analysis revealed a fixed composition of  $\text{SrFe}_{1-x}\text{Co}_x\text{O}_{3-\delta}$  with  $x = 0.38$  coexisting with Co-saturated  $\text{Sr}_4\text{Fe}_{4.4}\text{Co}_{1.6}\text{O}_{13\pm\delta}$  and Fe-saturated  $\text{Co}_{0.85}\text{Fe}_{0.15}\text{O}$ . The same method was used to determine the fixed composition of  $\text{Sr}_4\text{Fe}_{5.7}\text{Co}_{0.3}\text{O}_{13\pm\delta}$  coexisting with  $\text{Co}_{0.84}\text{Fe}_{2.16}\text{O}_4$  and  $\text{SrFe}_{12}\text{O}_{19-\delta}$  within the field 6 (Fig. 5).

#### 4. Conclusion

The solid solutions  $\text{SrFe}_{1-x}\text{Co}_x\text{O}_{3-\delta}$  ( $0 \leq x \leq 0.7$ ),  $\text{Sr}_3\text{Fe}_{2-y}\text{Co}_y\text{O}_{7-\delta}$  ( $0 \leq y \leq 0.4$ ),  $\text{Sr}_4\text{Fe}_{6-z}\text{Co}_z\text{O}_{13\pm\delta}$  ( $0 \leq z \leq 1.6$ ) have been prepared and their homogeneity ranges in air at 1100 °C have

**Table 4**

Phase composition within the fields of the cross-section of phase diagram of Sr-Fe-Co-O system (Fig. 5)

Fields on the diagram	Phase composition
1	$\text{CoO}$ , $\text{SrCoO}_{2.5\pm\delta}$ , $\text{SrFe}_{0.3}\text{Co}_{0.7}\text{O}_{3-\delta}$
2	$\text{Co}_{1-y}\text{Fe}_y\text{O}$ ( $0 \leq y \leq 0.15$ ), $\text{SrFe}_{1-x}\text{Co}_x\text{O}_{3-\delta}$ ( $0.38 \leq x \leq 0.7$ )
3	$\text{Co}_{0.85}\text{Fe}_{0.15}\text{O}$ , $\text{SrFe}_{0.62}\text{Co}_{0.38}\text{O}_{3-\delta}$ , $\text{Sr}_4\text{Fe}_{4.4}\text{Co}_{1.6}\text{O}_{13\pm\delta}$
4	$\text{Co}_{0.85}\text{Fe}_{0.15}\text{O}$ , $\text{Sr}_4\text{Fe}_{4.4}\text{Co}_{1.6}\text{O}_{13\pm\delta}$ , $\text{Co}_{1.38}\text{Fe}_{1.62}\text{O}_4$
5	$\text{Sr}_4\text{Fe}_{6-z}\text{Co}_z\text{O}_{13\pm\delta}$ ( $0.3 \leq z \leq 1.6$ ), $\text{Co}_u\text{Fe}_{3-u}\text{O}_4$ ( $0.84 \leq u \leq 1.38$ )
6	$\text{Sr}_4\text{Fe}_{5.7}\text{Co}_{0.3}\text{O}_{13\pm\delta}$ , $\text{Co}_{0.84}\text{Fe}_{2.16}\text{O}_4$ , $\text{SrFe}_{12}\text{O}_{19-\delta}$
7	$\text{Co}_{0.84}\text{Fe}_{2.16}\text{O}_4$ , $\text{SrFe}_{12}\text{O}_{19-\delta}$ , $\text{Fe}_{1.97}\text{Co}_{0.03}\text{O}_3$
8	$\text{SrFe}_{12}\text{O}_{19-\delta}$ , $\text{Fe}_{2-x}\text{Co}_x\text{O}_3$ ( $0 \leq x \leq 0.03$ ), $\text{SrFe}_{12}\text{O}_{19-\delta}$ , $\text{Sr}_4\text{Fe}_{6-z}\text{Co}_z\text{O}_{13\pm\delta}$ ( $0 \leq z \leq 0.3$ )
9	$\text{SrFe}_{12}\text{O}_{19-\delta}$ , $\text{Sr}_4\text{Fe}_{6-z}\text{Co}_z\text{O}_{13\pm\delta}$ ( $0 \leq z \leq 0.3$ )
10	$\text{Sr}_4\text{Fe}_{6-z}\text{Co}_z\text{O}_{13\pm\delta}$ ( $0 \leq z \leq 1.6$ ), $\text{SrFe}_{1-x}\text{Co}_x\text{O}_{3-\delta}$ ( $0 \leq x \leq 0.38$ )
11	$\text{SrFe}_{1-x}\text{Co}_x\text{O}_{3-\delta}$ ( $0 \leq x \leq 0.7$ ), $\text{Sr}_3\text{Fe}_{2-y}\text{Co}_y\text{O}_{7-\delta}$ ( $0 \leq y \leq 0.4$ )
12	$\text{SrFe}_{0.3}\text{Co}_{0.7}\text{O}_{3-\delta}$ , $\text{Sr}_3\text{Fe}_{1.6}\text{Co}_{0.4}\text{O}_{7-\delta}$ , $\text{Sr}_3\text{Co}_2\text{O}_{7-\delta}$
13	$\text{Sr}_3\text{Co}_2\text{O}_{7-\delta}$ , $\text{SrFe}_{0.3}\text{Co}_{0.7}\text{O}_{3-\delta}$ , $\text{SrCoO}_{2.5\pm\delta}$
14	$\text{SrO}$ , $\text{Sr}_3\text{Co}_2\text{O}_{7-\delta}$ , $\text{Sr}_3\text{Fe}_{1.6}\text{Co}_{0.4}\text{O}_{7-\delta}$
15	$\text{SrO}$ , $\text{Sr}_3\text{Fe}_{2-y}\text{Co}_y\text{O}_{7-\delta}$ ( $0 \leq y \leq 0.4$ )

been determined. The structural parameters of the solid solutions were refined by the Rietveld full-profile analysis and the isobaric-isothermal cross-section of the phase diagram for the Sr-Fe-Co-O system in air at 1100 °C has been constructed.

#### Acknowledgment

This work was financially supported by Russian Foundation for Basic Researches (Project RFBR-Urals N 07-03-96079).

#### References

- U. Balachandran, T.J. Dusek, S.M. Sweeney, R.B. Poeppel, R.L. Mievil, P.S. Maiya, M.S. Kleefisch, S. Pei, T.P. Kobylinski, C.A. Udovich, A.C. Bose, *Am. Ceram. Soc. Bull.* 74 (1995) 71–75.
- H. Fjellvåg, B.C. Hauback, R. Bredesen, *J. Mater. Chem.* 7 (1997) 2415–2419.
- W. Jin, I.R. Abothu, R. Wang, T.-S. Chung, *Ind. Eng. Chem. Res.* 41 (2002) 5432–5435.
- Z.Q. Deng, W. Liu, D.K. Peng, C.S. Chen, W.S. Yang, *Mater. Res. Bull.* 39 (2004) 963–969.
- B. Ma, J.P. Hodges, J.D. Jorgensen, D.J. Miller, J.W. Richardson, U. Balachandran, *J. Solid State Chem.* 141 (1998) 576–586.
- L. Mogni, F. Prado, A. Caneiro, *Chem. Mater.* 18 (2006) 4163–4170.
- G.M. Veith, R. Chen, G. Popov, M. Croft, Y. Shokh, I. Nowik, M. Greenblatt, *J. Solid State Chem.* 166 (2002) 292–304.
- S. Ghosh, P. Adler, *J. Mater. Chem.* 12 (2002) 511–521.
- A. Maignan, C. Martin, N. Nguyen, B. Raveau, *Solid State Sci.* 3 (2001) 57–63.
- P.D. Battle, M.A. Green, J. Lago, A. Mihut, M.J. Rosseinsky, L.E. Spring, J. Singleton, J.F. Ventre, *Chem. Commun.* (1998) 987.
- A. Fossdal, L.T. Sagdahl, M.-A. Einarsrud, K. Wiik, T. Grande, P.H. Larsen, F.W. Poulsen, *Solid State Ionics* 143 (2001) 367–377.
- S. McIntosh, J.F. Vente, W.G. Haije, D.H.A. Blank, H.J.M. Bouwmeester, *Solid State Ionics* 177 (2006) 833–842.
- N. Grunbaum, L. Mogni, F. Prado, A. Caneiro, *J. Solid State Chem.* 177 (2004) 2350–2357.
- A. Fossdal, M.-A. Einarsrud, T. Grande, *J. Solid State Chem.* 177 (2004) 2933–2942.
- M. Takano, T. Okita, N. Nakayama, Y. Bando, Y. Takeda, O. Yamamoto, J.B. Goodenough, *J. Solid State Chem.* 73 (1988) 140–150.
- L. Fournès, Y. Potin, J.C. Grenier, G. Demazeau, M. Pouchard, *Solid State Commun.* 62 (1987) 239–244.
- A. Wattiaux, L. Fournès, A. Demourgues, N. Bernabén, J.C. Grenier, M. Pouchard, *Solid State Commun.* 77 (1991) 489–493.
- M. Schmidt, *J. Phys. Chem. Solids* 61 (2000) 1363–1365.
- T.C. Gibb, *J. Chem. Soc. Dalton Trans.* (1985) 1455–1470.
- H. Taguchi, *J. Mater. Sci. Lett.* 2 (1983) 665–666.
- J.-C. Grenier, N. Ea, M. Pouchard, P. Hagenmuller, *J. Solid State Chem.* 58 (1985) 243–252.
- S.E. Dann, M.T. Weller, D.B. Currie, *J. Solid State Chem.* 92 (1991) 237–240.
- K. Mori, T. Kamiyama, H. Kobayashi, S. Torii, F. Izumi, H. Asano, *J. Phys. Chem. Solids* 60 (1999) 1443–1446.
- O. Pérez, B. Mellenne, R. Retoux, B. Raveau, M. Hervieu, *Solid State Sci.* 8 (2006) 431–443.

- [25] M.D. Rossell, A.M. Abakumov, G. Van Tandeloo, M.V. Lomakov, S.Ya. Istomon, E.V. Antipov, *Chem. Mater.* 17 (2005) 4717–4726.
- [26] X. Obradors, X. Solans, A. Collomb, D. Samaras, J. Rodriguez, M. Pernet, M. Font-Altaba, *J. Solid State Chem.* 72 (1988) 218–224.
- [27] K. Kimura, M. Ohgaki, K. Tanaka, H. Morikawa, F. Marumo, *J. Solid State Chem.* 87 (1990) 186–194.
- [28] S.K. Rakshit, S.C. Parida, S. Dash, Z. Singh, R. Prasad, V. Venugopal, *Mater. Res. Bull.* 40 (2005) 323–332.
- [29] T. Takeda, H. Watanabe, *J. Phys. Soc. Japan* 33 (1972) 973–978.
- [30] Y. Xia, T. Armstrong, F. Prado, A. Manthiram, *Solid State Ionics* 130 (2000) 81–90.
- [31] Z. Deng, G. Zhang, W. Liu, D. Peng, C. Chen, *Solid State Ionics* 152–153 (2002) 735–739.
- [32] N.V. Proskurnina, V.A. Cherepanov, O.S. Golynets, V.I. Voronin, *Inorg. Mater.* 40 (2004) 955–959.
- [33] R.D. Shannon, C.T. Prewitt, *Acta Crystallogr. A* 32 (1976) 751–753.